Evaluation of the Fate of Nitrate and Analysis of Shallow Soil Water using Geo-electrical Resistivity Survey

Nur Islami

Department of Physics Education, FKIP, Universitas Riau
Jalan H.R. Soebrantas Km 12.5 Simpang Baru, Pekanbaru 28293, Indonesia
E-mail: nurislami@lecturer.unri.ac.id

Abstract. Evaluation of the fate of nitrate and analysis of shallow soil water in a tobacco plantation area were conducted using integration of soil properties and hydrogeochemical analysis, and geo-electrical resistivity methods, taking measurements four times within a three-month period. The sampling data were taken in two areas: a fertilized and a nonfertilized zone. Chemical fertilizer was introduced to the fertilized zone after the first data acquisition. Hydrogeohemical analysis of the soil water was conducted from the surface to a depth of 1 m at an interval of 25 cm. The results show that the cations in the soil water were quite comparable for each monitoring time. Conversely, relatively larger changes in anion content occurred at the surface until a depth of 1 m. In particular, the nitrate concentration reached its maximum level at about 67 days after fertilization and returned to its initial value approximately 195 days after fertilization. The geo-electrical resistivity profiles exhibited no indication of low resistivity values prior to fertilization near the surface. However, lower resistivity values were found in the fertilized zone at the second and third measurement. The result shows that the adjoining environment dissolved the nitrate concentration in the pore soil within the three-month time period.

Keywords*: bachok; fate of nitrate; geo-electrical resistivity; hydrogeochemical; tobacco.*

1 Introduction

Chemical fertilizers are used extensively to enhance agricultural productivity in farmed areas. Shallow groundwater pollution is a significant impact of farming industry practices using large amounts of chemical fertilizers. The impact of using chemical fertilizers on shallow subsurface water has been studied by Zao, *et al*. [1] and Peria, *et al*. [2], among others. Zao, *et al*. reported that nitrate accumulation was found in the near surface soil profile from five different long-term fertilization sites [1]. A relatively higher accumulation of nitrate was dominant at the site where inorganic fertilizer had been used compared to sites with manure input as fertilizer. Furthermore, increasing the inorganic fertilizer with N components (such as NPK) caused a drastic increase of nitrate in the soil. Peria, *et al*. [2] have shown that the rate of nitrate concentration in shallow

Received October 6th, 2016, 1st Revision February 25th, 2017, 2nd Revision April 16th, 2017, 3rd Revision 11th, 2017, Accepted for publication October 17th, 2017.
 ISSN: 2337-5779, DOI: 10.5614/j.eng.technol.sci.2017.49.4.5

groundwater, besides depending on the amount of inorganic fertilizer, is also subject to crop type and environmental conditions such as groundwater flow and organisms living on the site.

Investigations into various sources of nitrate in groundwater have been done by several researchers. The source of nitrate in groundwater can be local agricultural activities but also transportation processes from other locations [3,4]. The direction of the surface water and groundwater flow definitely influence the nitrate concentration in the ending zone of the water flow and in the initial water resources. A study on chemical and resistivity characteristics of agricultural soil in a semi-pervious aquifer has been carried out by Islami, *et al*. [5], which showed a resistivity and hydrogeochemical contrast between an area that was applied with fertilization for a long duration and a non-fertilized area. Youngsun, *et al*. [6] reported a study on mitigation of nitrate discharge from rigorous crop farming in the Haean catchment, South Korea. Leaching of nitrate was recognized as the dominant pathway of N loss, leading to substantial indirect N_2O emissions and threats to water quality. The reduction of fertilizer practices showed a high potential of decreasing N_2O emission and nitrate leaching [6]. Otero, *et al*. [7] conducted a study on the monitoring of nitrate using a multi-isotope method, which provides an approximation of the degree of natural attenuation of nitrate. The result showed clear denitrification and contaminant diminution in the groundwater. Yan, *et al*. [8], Al-Charideh, *et al*. [9] and Karan, *et al*. [10] have tried to trace the source of nitrate pollution using isotope analysis. These studies showed that fertilizer application, precipitation, and irrigation strongly influence nitrate concentrations in surface water. Furthermore, analyses of isotopic compositions have shown that the sources of nitrate are mainly nitrification processes of fertilizer and manure in surface water. In the wet season, application of fertilizers to the ground will cause transportation of nitrate by precipitation through the soil layers and to the groundwater. Meanwhile, denitrification only occurs in surface water during the wet season [10].

The geo-electrical resistivity method has been widely used in subsurface exploration. It was used to investigate subsurface topography by Kneisel, *et al*. [11] and Tsokas, *et al*. [12], among others. Kneisel, *et al*. employed 3D geo-electrical resistivity imaging for mapping frozen ground conditions. 3D geo-electrical imaging enables spatial imaging of the subsurface resistivity distribution and shows improvement of the delineation of frozen ground structure characteristics. Furthermore, a geo-electrical resistivity survey can be used to image the foundations of ancient walls, especially in employing cross-hole resistivity [12]. This method has been examined in engineering, especially for the construction aspect. A higher correlation between decreasing resistivity and the diffusivities of chloride is a good indicator of concrete durability [13].

The effects of specimen parameters such as correction coefficient K (the ratio between specimen length and diameter to the probe spacing) and moisture content of concrete have the highest impact on resistivity [14]. Resistivity has also been proved as an important indicator for possible risks involved in hydraulic piping or tunneling in earth-works and constructions such as road embankments, and degree of compaction after the correlation between the electrical resistivity of a non-cohesive soil and the degree of compaction was determined [15]. The effectiveness of using the geo-electrical resistivity method to explore a number of geo-environmental problems has been well established in several case studies. Khaki, *et al*. [16] have shown that the fresh and brackish-water interface in coastal areas can be clearly represented using geo-electrical resistivity survey. A study on the contamination of groundwater by CO_2 leaking is reported in Esben, *et al*. [17]. Geo-electrical resistivity can detect and image dissolved CO_2 in a shallow aquifer with a fully automated acquisition system that sends the data to an online database. 3D time-lapse resistivity inversions clearly image the dissolved CO_2 plume with decreased resistivity values [17]. Geo-electrical resistivity surveys have also been used to study groundwater contamination due to uncontrolled landfill leachate occurring rapidly and extensively following the rainy season [18]. The electrical resistivity values of contaminated zones are relatively lower than those of uncontaminated zones. This is due to an abundance of ions or molecules in the groundwater that can easily transfer electric current [18].

Conversely, no work has been reported on the use of geo-electrical resistivity survey to evaluate the fate of nitrate with particular soil conditions in tobacco plantation areas. Furthermore, geo-electrical imaging survey has seldom been combined together with chemical analysis of soil pore water samples and soil property analysis. In this paper, application of soil property analysis, hydrogeochemical and geo-electrical resistivity surveys for the monitoring of the fate of nitrate in the near-surface zone of fine-grained sandy soil are presented. The evaluation of nitrate in groundwater as a result of chemical fertilizer usage is important because the U.S. Environmental Protection Agency has suggested that the maximum nitrate concentration in water for drinking is 45 mg/L [19]. Groundwater is the principal resource of drinking water for the community in the study area.

2 Material and Methods

In the study area, tobacco plantation is the major cultivation activity. Farming is done by the local community. To enhance the tobacco productivity, like in other places, chemical fertilizers are used extensively. The tobacco plantation activities begin in the middle of January and end in the middle of April every year since a couple of decades. For the rest of the year (May-December), some

farmers plant other crops, such as corn, chili, and others. The plants (excluding tobacco) need 200 kg of urea (40% of nitrogen content) of chemical fertilizer per 1 ha during a planting period of 3 months. The fertilization scheme for tobacco is quite simple: the tobacco plants needs only 200 kg of particular fertilizer per ha for one planting season. The fertilizer that is used for tobacco plants consist of the following materials: N: 10%, P_2O_3: 2%, K_2O: 2%, MgO: 0.5%, SiO_2: 9%, Ca: 2%, organic carbon: 30%, and moisture: 20% (personal communications).

An infertile site of a former tobacco plantation in Bachok, Malaysia (6°04'10.76" N; 102°23'37.39" E) was selected as the investigation area. This site was chosen because it is no longer used for tobacco plantation, so there had been no fertilization activity before the survey was conducted. The study area is dominated and covered by marine deposits due to its vicinity to the beach line at a distance of approximately 800 m [20].

A series of measurements was conducted in different survey phases. All the procedures were acclimatized naturally, including maintaining an undisturbed biological environment, watering by rainfall, and application of chemical fertilizer using the regular rule. Data collection was performed within a three-month period, from June to September, 2015. The first (14 Jun 2015), second (05 Jul 2015), third (02 Aug 2015) and fourth measurements (25 Sep 2015) are referred to as first monitoring (M-1), second monitoring (M-2), third monitoring (M-3), and forth monitoring (M-4), respectively. The survey arrangement can be seen in Figure 1.

Soil grain size distribution, hydraulic conductivity and soil pore water were measured to obtain soil and pore soil water characterization. Soil samples were collected from the surface level and to a depth of 100 cm for every 25 cm using a hand auger. The samples were dried in an oven at a temperature of 105 °C for 24 hours prior to sieving. The dried soil was sieved and classified in terms of grain size, i.e. gravel, sand, silt, and clay, respectively [21]. The soil moisture content of the soil samples was determined using the weight reduction method on the soil before and after drying. The hydraulic conductivity of the soil was measured at the site using the inverse auger hole method [22], which is obtained from analyzing the water level decrease over time in a hole filled with water (11.5 cm in diameter and 60 cm deep). A 1900 Soil Water Sampler from Equipment Corp. USA was used as soil moisture extraction equipment to collect soil pore water (water in the vadoze zone) at a certain depth. The water samples obtained from the site were stored at a temperature of 4 °C in a thermos container with ice inside, waiting to be sent to the hydrogeology laboratory for chemical determination analysis of anions and cations using inductively coupled plasma (ICP) and ion chromatography (IC) because of the speed, precision, and

sensitivity of these methods [23]. In order to analyze the water samples using ICP, additional acid within the water samples was required to achieve a pH level of 4 [30]. This pH level is mandatory to protect the samples from reactions before processing in the laboratory.

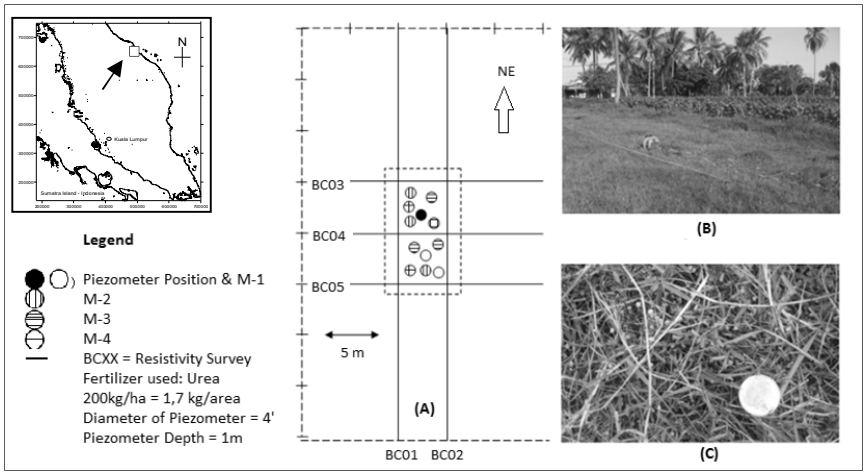

Figure 1 (A) Field setup, (B) view around the survey site, (C) fertilizer introduction after M-1. The coordinates of the piezometer were 6°04'10.76" N and 102°23'37.39" E.

Geo-electrical resistivity survey was used to detect the electrical property changes of the soil. A DC current was injected through an electrode and received by a second current electrode. Two potential electrodes were then employed to detect the voltage difference between both points. The amount of electrical current injected into the ground is influenced by several factors: type of soil matrix mineral and fluid in the pore soil. If the injected current and voltage are measured and the distance between both electrodes is known, the resistivity value of the subsurface can be determined [25]. 2D geo-electrical resistivity imaging survey was performed on two lines with 0.5 m of electrode spacing and a length of 40 m for a northeast-southwest direction. Another survey was conducted in a west-south direction on three lines perpendicular to the first two lines, with a length of 20 m due to lack of space. Each line was separated by a space of 5 m. At the site it was possible to conduct gridded-line surveys on 6 lines in a northeast-southwest direction and 9 lines in a southeast-northwest direction. However, data acquisition takes more than one day. This will lead to differences in the soil moisture content due to the evaporation process and hence differences in the resistivity readings. The apparent resistivity data obtained from the surveys were processed using Res2Dinv software [25] to produce the true subsurface resistivity profile. 1.7 kg of

fertilizer (equal to 200 kg per ha) was distributed over the whole fertilizer zone (7 x 12 m) after the first measurement (M-1).

3 Results and Discussion

3.1 Soil and Hydraulic Conductivity Characteristics

The soil distribution and depth for each hole sample are given in Figure 2. The highest percentage of fine sand was obtained at a depth of 25 cm (97%) and found in all sampling locations at the same depth. Fine sand grain is a dominant grain with no specific trend. Meanwhile, coarse sand and gravel were absent. The highest medium sand grain percentage (8%) was observed in the near-surface zone. Silt and clay ranged from 1.98 to 3.11%. Generally, the same trend of grain size distribution occurred for all sampling locations. The inverse auger method was used to measure hydraulic conductivity at shallow depths above water level. The hydraulic conductivity for the site was 0.00211 cm/s, which was obtained from the graph of water level (ht + r/2) versus time. Based on grain soil analysis and hydraulic conductivity analysis, the soil condition is suitable for an aquifer and is within semi-pervious and pervious soil characters [26].

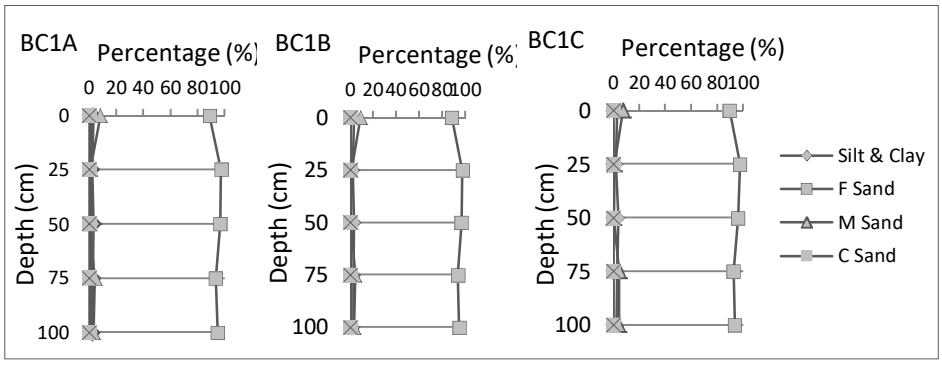

Figure 2 Grain size distributions with depth.

3.2 Moisture Content

Graphs of sampling depth versus moisture content for different monitoring periods and rainfall data within the survey period are given in Figures 3 and 4, respectively. The lowest amount of moisture content was observed in the near-surface zone, and it increased with depth. The lower moisture content is due to the evaporation process as a result of sunlight directly shining on the surface. A similar trend was observed in all monitorings, except in M-4. In M-4, at a depth

greater than 25 cm, the moisture content did not drastically increase as was the case for the other monitoring data because there had been no heavy rainfall in the days before M-4.

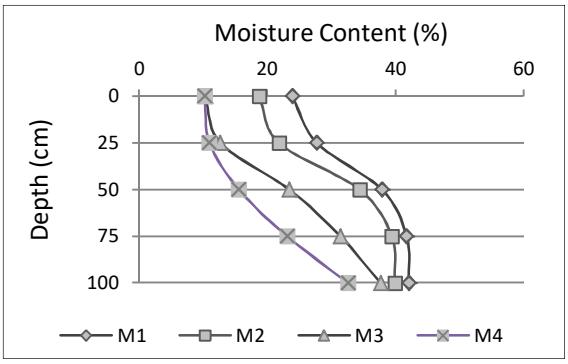

Figure 3 Graph of sampling depth versus moisture content for each monitoring.

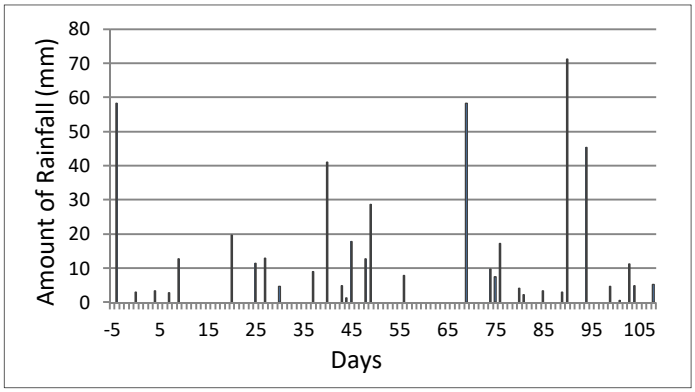

Figure 4 Rainfall data within survey period.

Fine and medium sand grains dominated in the near-surface layer. In terms of grain size distribution, the soil in the near-surface layer had relatively good porosity and permeability as predicted from the hydraulic conductivity analysis. Additionally, pore soil water content (soil moisture) was subjected by rainfall quantity and length of time before the soil sample was taken. M-1 showed the highest amount of moisture content and, generally, pore soil water content increased with increasing depth in each survey.

3.3 Chemical Content of Extracted Soil Water

The chemical contents of the pore soil water for each survey are given in Table 1. Generally, Ca, Mg and Na increased with depth. This is because the site is

located in a marine deposit environment. Residual cation content from seawater still remains in the soil. However, all cation contents are still within human consumption tolerance [27].

Table 1 Chemical content of extracted water for each monitoring.

M	Depth (cm)	Chlorid mg/L	Nitrate mg/L	Sulphate mg/L	Fluoride mg/L	K mg/L	Ca mg/L	Mg mg/L	Pb mg/L
1	BCM1-0	21.60	21.40	10.00	0.20	20.28	93.86	34.36	0.00
	BCM1-25	26.80	19.80	12.80	0.00	22.46	97.52	39.10	0.02
	BCM1-50	23.00	18.40	27.60	0.20	16.68	101.86	42.50	0.00
	BCM1-75	25.20	15.20	30.20	0.40	17.73	108.90	45.68	0.00
	BCM1-100	31.00	7.60	41.10	0.00	17.24	108.48	51.70	0.01
	Mean	25.52	16.48	24.34	0.16	18.88	102.12	42.67	0.01
2	BCM2-0	178.00	71.00	183.60	0.20	19.26	94.82	36.52	0.06
	BCM2-25	119.40	56.40	160.40	1.20	20.10	97.66	35.84	0.00
	BCM2-50	102.40	41.60	140.80	0.60	22.38	98.20	39.96	0.00
	BCM2-75	97.40	26.00	132.40	0.20	20.70	105.14	42.20	0.02
	BCM2-100	96.80	23.40	132.20	0.20	19.78	103.88	49.78	0.00
	Mean	118.80	43.68	149.88	0.48	20.44	99.94	40.86	0.02
3	BCM3-0	121.60	171.00	110.40	0.20	19.39	88.05	34.96	0.00
	BCM3-25	101.00	328.40	102.20	0.20	21.27	87.27	33.67	0.01
	BCM3-50	90.00	126.00	106.60	0.60	18.72	90.36	36.91	0.01
	BCM3-75	87.60	46.40	104.40	0.00	16.40	90.16	45.64	0.04
	BCM3-100	98.20	42.20	101.80	0.60	16.46	98.84	49.18	0.00
	Mean	99.68	142.80	105.08	0.40	18.45	90.94	40.07	0.01
4	BCM4-0	110.00	110.60	77.00	0.20	19.48	91.98	36.64	0.01
	BCM4-25	94.00	102.40	77.80	0.00	21.41	112.94	42.46	0.00
	BCM4-50	98.40	106.20	81.20	0.00	18.11	94.88	41.42	0.02
	BCM4-75	92.00	52.40	81.60	0.00	16.73	100.08	46.88	0.00
	BCM4-100	99.20	49.00	87.00	0.00	15.44	87.04	53.00	0.00
	Mean	98.72	82.92	80.92	0.20	18.23	97.38	44.08	0.01

M	Depth (cm)	Cd mg/L	Se mg/L	Al mg/L	Mn mg/L	Cu mg/L	Zn mg/L	Fe mg/L	As mg/L	Na mg/L
1	BCM1-0	0.00	0.01	0.08	0.00	0.05	0.00	0.20	0.00	29.72
	BCM1-25	0.00	0.01	0.00	0.01	0.04	0.00	0.00	0.00	28.44
	BCM1-50	0.00	0.02	0.05	0.04	0.05	0.01	0.30	0.00	30.54
	BCM1-75	0.00	0.02	0.00	0.10	0.03	0.00	0.00	0.00	36.16
	BCM1-100	0.00	0.02	0.00	0.03	0.02	0.00	0.00	0.00	37.12
	Mean	0.00	0.01	0.03	0.04	0.04	0.00	0.10	0.00	32.40
2	BCM2-0	0.00	0.01	0.08	0.03	0.14	0.03	0.20	0.00	27.96
	BCM2-25	0.00	0.00	0.00	0.00	0.00	0.00	0.00	0.00	28.62
	BCM2-50	0.00	0.04	0.03	0.06	0.03	0.00	0.00	0.00	28.50
	BCM2-75	0.00	0.02	0.00	0.08	0.02	0.00	0.00	0.00	33.73
	BCM2-100	0.00	0.01	0.00	0.02	0.01	0.00	0.02	0.00	37.14
	Mean	0.00	0.02	0.02	0.04	0.04	0.01	0.05	0.00	31.19
3	BCM3-0	0.00	0.01	0.04	0.04	0.06	0.00	0.04	0.00	28.49
	BCM3-25	0.00	0.01	0.06	0.02	0.07	0.00	0.01	0.00	26.41
	BCM3-50	0.00	0.01	0.02	0.05	0.02	0.03	0.14	0.00	29.74
	BCM3-75	0.00	0.01	0.03	0.01	0.01	0.00	0.11	0.00	34.93
	BCM3-100	0.00	0.02	0.00	0.00	0.02	0.01	0.00	0.00	34.86
	Mean	0.00	0.01	0.03	0.02	0.04	0.01	0.06	0.00	30.88
4	BCM4-0	0.00	0.02	0.00	0.12	0.06	0.02	0.03	0.00	28.43
	BCM4-25	0.00	0.01	0.00	0.20	0.01	0.02	0.00	0.00	28.17
	BCM4-50	0.00	0.03	0.00	0.00	0.02	0.00	0.12	0.00	30.15
	BCM4-75	0.00	0.01	0.00	0.00	0.03	0.00	0.02	0.00	32.49
	BCM4-100	0.00	0.01	0.00	0.01	0.01	0.00	0.11	0.00	35.69
	Mean	0.00	0.02	0.00	0.07	0.03	0.01	0.06	0.00	30.99

In M-1, the highest average of anion content was chloride (25.52 mg/L), followed by sulphate (24.34 mg/L), nitrate(16.48 mg/L) and fluoride (<1 mg/L). The maximum chloride content (31.00 mg/L) was obtained at the largest depth. The chloride concentration increased with depth. Sulphate had the same trend as chloride.

The nitrate concentration was highest in the near-surface layer and decreased with depth. Fluoride had no a specific trend. Existence of chloride and sulphate was predicted due to the residual marine deposit. Meanwhile, the relatively high nitrate concentration was due to animal manure that covered most of the ground surface. However, all anion contents in the water samples were still within human consumption tolerance [27].

In M-2, the cation content in the water samples was similar to M-1. However, the anion content showed a significant difference with M-1. The maximum chloride, nitrate and sulphate content in the pore soil water (178.00, 71.00 and 183.60 mg/L, respectively) was found at the surface. Chloride, nitrate and sulphate content was observed to decrease with depth. The effect of introduced fertilizer immediately after the first acquisition was quite obviously seen in the pore soil water content.

In M-3, the highest nitrate concentration (328.40 mg/L) was obtained at a sampling depth of 25 cm. It reduced progressively. The nitrate concentration was higher than in M-2. Meanwhile, the maximum value of chloride (121.60 mg/L) was observed on the surface. It dropped slowly with increasing depth. The same trend was also recognized for the sulphate concentration, of which the highest (110.40 mg/L) value was at the near surface. The average chloride (99.68 mg/L) and nitrate (142,8 mg/L) contents were approximately 0.83 and 3.26 times higher respectively compared to M-2. The cation concentration was almost identical to M-1 and M-2.

M-4 was the last measurement in this study. The highest nitrate concentration (110.60 mg/L) was obtained at the surface. It decreased progressively with increasing depth. However, at the two largest sampling depths (75 and 100 cm), the nitrate content in the pore soil was higher than in M-2. The highest chloride concentration (110.00 mg/L) was observed in the near-surface layer. It decreased at 25 cm sampling depth and increased slowly with depth. This trend was also noted for the sulphate concentration. In general, the cations of the pore soil water were almost identical for each monitoring. Figure 5 shows the average concentration of anion content in the water samples ranging from 0 cm to 100 cm depth and the near-surface layer (0-25 cm) for each monitoring.

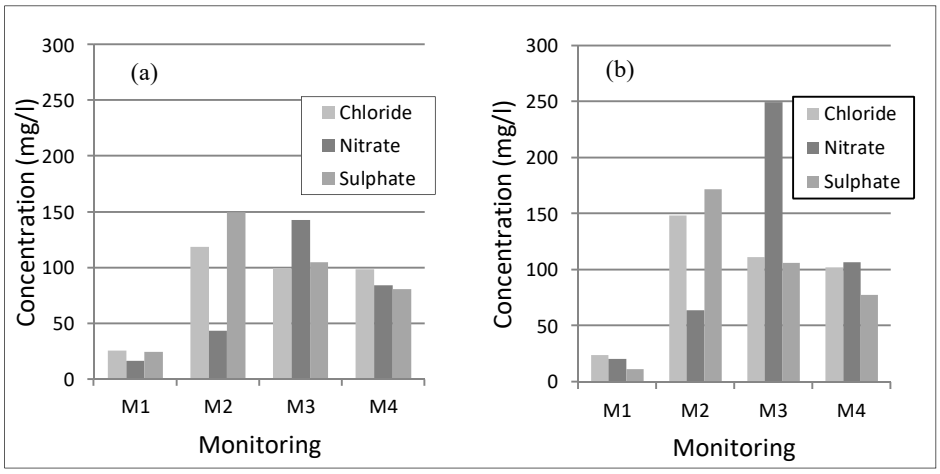

Figure 5 Average concentration of anion content ranging from 0 to 100 cm depth (a) and from 0 to 25 cm depth versus monitoring (b).

3.4 Geo-electrical Resistivity Model

The geo-electrical resistivity models for each survey are given in Figure 6.

1. **M-1**

   In the geo-electrical resistivity of BC11, the highest resistivity value (> 250 ohm.m) occurred in the near-surface layer, especially towards the half-right side of the section. This value was supported by surface measurements of soil resistivity at ten random locations with an average of 176.80 ohm.m (62.42 ohm.m standard deviation). This corresponds to fine sand with low moisture content. In the profile of line BC12, the same resistivity value pattern as for line BC11 was observed near the surface. A resistivity value of approximately 50 ohm.m was obtained at depths of 1.10 to 2.50 m, corresponding to the zones with freshwater content. At larger depths, ranging from 2.50 to 4.50 m, the resistivity value was relatively higher, correlating to a less porous zone filled with freshwater. On the right side at the same depth, a relatively higher resistivity value (120 ohm.m) was observed correlating to a more compacted material.

   The material continues in a southeast-northwest direction (perpendicular to both lines). The continuity of the material was disturbed around the 16 to 20 m mark, but it could still be found on the left side of the section, which had higher porosity. In the deepest part of this section (> 5.5 m), the lowest resistivity value (less than 8 ohm.m) was observed, corresponding to brackish water. In the geo-electrical model along lines BC13, BC14 and

BC15, a similar resistivity value pattern was observed in the other three geo-electrical models.

2. **M-2**

Along lines BC21 and BC22, the resistivity profile pattern was almost identical to M-1 except at the location where chemical fertilizers had been introduced (14.5 to 25.5 m mark). In the fertilization zone, the resistivity value decreased drastically. In the geo-electrical model along line BC21, up to the 14.5 m mark, the average surface resistivity value was 156.01 ohm.m (derived from geo-electrical model extraction).

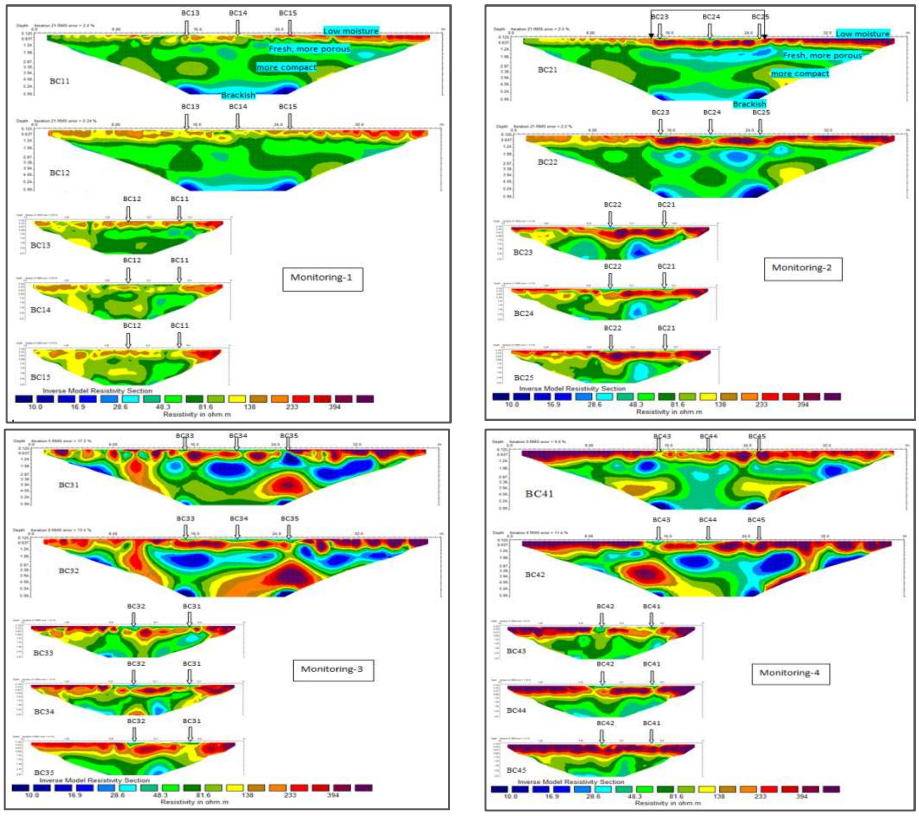

Figure 6 Geo-electrical model of M-1, M-2, M-3 and M-4.

The average surface resistivity value for the fertilized zone was 56.54 ohm.m. Meanwhile, after the 25.5 m mark the average resistivity value was 667.12 ohm.m. These values were supported by direct resistivity measurement, which was 52.02 ohm.m inside the fertilized zone and 400.71 ohm.m outside of the fertilized zone. For the record, the average surface

resistivity for BC11 (M-1) in the same zone was 123.98, 169.07 and 332.27 ohm.m. On the four other lines decreasing trends of resistivity were also found in the fertilized zone, like for line BC21. Below the fertilized zone on line BC21, a lower resistivity value was found at a depth of 1.2 to 2.5 m when compared to the left and right side of the section, which were unfertilized. This trend was also found for the other lines (BC22, BC23, BC24 and BC25).

3. **M-3**

   In M-3, an average surface resistivity value of 386.03 ohm.m was observed from the beginning of the line to the 14.5 m mark (line BC31). Meanwhile, in the fertilized zone the average resistivity value was 44.23 ohm.m. After the 25.5 m mark the average resistivity value was 718.72 ohm.m. This value was derived from geo-electrical model extraction. The same trend of the resistivity value was also found for the other four lines. The path of materials leaking downward from the surface can be clearly seen in the 24.5 m mark zone. A high concentration of anions moving through this path to a deeper level is clearly visible. Compared to BC21 at the same depth location (24;1.5), BC31 showed a decrease in resistivity that is proportional to the increase in nitrate content. Other lines also showed similar trends of decreasing resistivity value due to increased nitrate concentration.

4. **M-4**

   In the geo-electrical model along line BC41, a similar resistivity pattern near the surface was still observed as occurred in the previous monitoring. At locations where chemical fertilizers were introduced (14.5 to 25.5 m mark), a lower resistivity value could still be found. On line BC41, up to the 14.5 m mark, the average resistivity value was 305.764 ohm.m, while in the fertilized zone it was 92.364 ohm.m. Compared to the two previous monitorings, the geo-electrical model for M-4 (BC41) showed a resistivity value of about 14 ohm.m at a depth of around 2.3 m. In the previous monitoring, the resistivity value was more than 14 ohm.m within this zone. This was probably caused by leaching of the chemical fertilizer anion content from the surface due to the rainfall. Furthermore, it could also have been caused by anion content from the brackish water moving up through the capillarity process as an impact of a low input of freshwater from rainfall.

3.5 Fate of Nitrate

Graphs of nitrate concentration versus time and nitrate concentration versus sampling depth are given in Figures 7 and 8, respectively. In Figure 7 it can be

seen that the highest nitrate concentration occurred on the surface, except at a depth of 25 cm. This happened 49 days after introducing the chemical fertilizer. Meanwhile, for depths of 50, 75 and 100 cm, the highest value occurred in the last survey (on the 103th day). In Figure 8, the nitrate content of the soil water increased considerably in M-2 over the entire sampling depth. On average, it increased 3.47 times compared to M-1 and decreased with depth almost linearly. Other researchers [24,29] have stated that the amount of nitrate leaching is also affected by water flux and moisture content of the soil. The rainfall data (Figure 4) were obtained from *Pejabat Pusat Pertanian Bachok* and show that the quantity of water in the time intervals between M-1 and M-2, M-2 and M-3, M-3 and M-4, was 22.4 mm, 123.4 mm, 289.3 mm, respectively. Other water inputs such as artificial irrigation were not applicable in the study area. Rainfall occurred between each monitoring, making significantly more water present in the pore soil, especially at a depth of more than 50 cm (Figure 3). However, at a depth of 0 to 25 cm, the amount of water in the pore soil remained relatively low. This was due to the soil condition being on the borderline of pervious and semi-pervious soil. Based on Figures 4, 7 and 8, there is no relation between the amount of nitrate in the top soil and the rate of rainfall and the moisture content. However, Lee [24] reported that the Nitrosomonas bacteria has an important influence on the fate of nitrate (in this paper the effect of this bacteria is not questioned). Finally, based on the trend of nitrate content found in sallow soil water, the fate of the nitrate concentration (N) in the near surface can be predicted using the fitting method as in Eq. (1):

$$\mathrm{N} = (\alpha + \beta.\mathrm{D})/(1 - \gamma.\mathrm{D} + \delta.D^2) \quad (1)$$

Here, α is the nitrate content (mg/L) in the soil water before fertilizer application, while β, γ and δ are constants with a value of 0.2990, 0.0260 and 0.0002, respectively. Lastly, D is the day of monitoring. Prediction of the fate of nitrate on the surface using Equation 1 was compared with the measured nitrate content, plotted together in Figure 9. It can be seen that the predicted and measured nitrate concentration had a correlation of 0.9970.

Based on the graph in Figure 9, the nitrate concentration is predicted to reach its maximum level approximately on day 67 and to return to its initial value on day 195. Meanwhile, at another location (a palm oil plantation) with a different soil grain and environmental conditions, the maximum nitrate concentration was reached on day 36 after fertilization [28]. Although the amount of urea introduced in the studied site was 0.67 times less than in the palm oil plantation, it has a long life and the peak growth of nitrate was 2 times and 1.4 times higher respectively than in the palm oil plantation. This result shows that the soil characteristics and the presence of Nitrosomonas bacteria [24] are probable as important factors affecting the fate of nitrate.

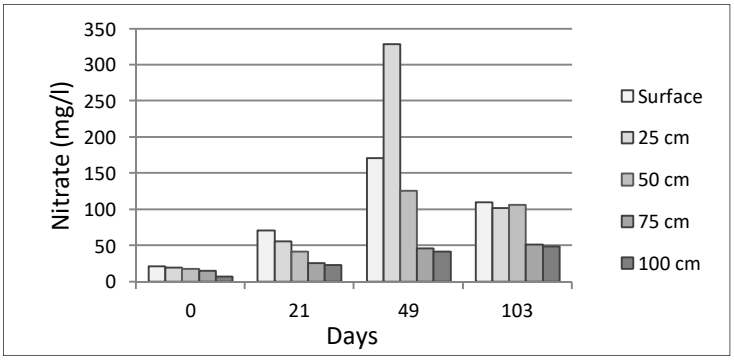

Figure 7 Nitrate concentration versus survey time (days) for each depth.

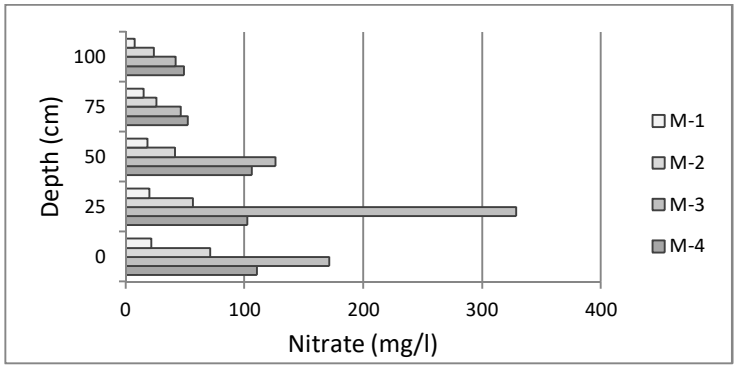

Figure 8 Amount of nitrate in soil water versus depth for each survey.

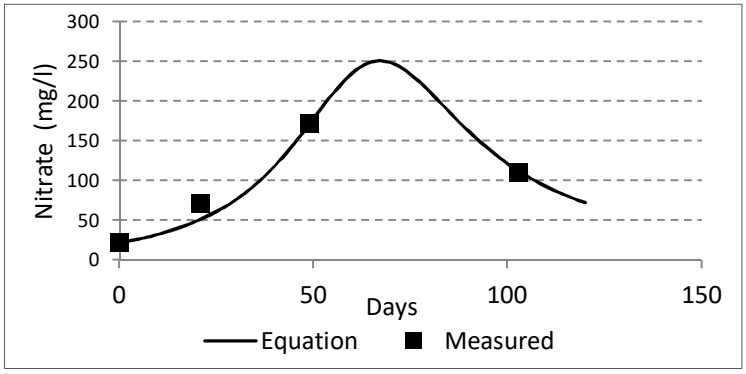

Figure 9 Amount of nitrate at the near surface in soil water for each survey.

4 Conclusion

Soil property and hydrogeochemical analysis, and geo-electrical resistivity survey were successfully used to monitor and evaluate the fate of nitrate in the sandy soil of a former tobacco plantation area. The hydrogeochemical measurements indicate that the cation content was relatively similar at each monitoring time. However, relatively higher changes of anion content occurred in the near-surface zone. The geo-electrical model prior to fertilization showed a similar resistivity value in the near-surface zone with no significant of low resistivity value. Lower resistivity values occurred during the second, third and fourth monitoring in the fertilized zone. An equation for the growth of nitrate was derived, which can be used to predict the lifetime and peak growth of the nitrate concentration after fertilization in the near-surface layer.

Acknowledgments

The author would like to thank to Department of Geology, University of Malaya for the series of part-time Research Collaborations since 2012.

References

[1] Zhao, B.Q., Li, X.Y., Liu, H., Wang, B.R., Zhu, P., Huang, S.M., Bao, D.J., Li, Y.T. & So, H.B., *Results from Long-Term Fertilizer Experiments in China: The Risk of Groundwater Pollution by Nitrate*, NJAS-Wageningen Journal of Life Sciences, **58**(3-4), pp. 177-183, 2011.

[2] Peña-Haro, S., Llopis-Albert, C., Pulido-Velazquez, M. & Pulido-Velazquez, D., *Fertilizer Standards for Controlling Groundwater Nitrate Pollution from Agriculture: El Salobral-Los Llanos Case Study, Spain*, Journal of Hydrology, **392**(3-4), pp. 174-187, 2010.

[3] Murgulet, D. & Tick, G.R., *Understanding the Sources and Fate of **Nitrate** in a Highly Developed Aquifer System,* Journal of Contaminant Hydrology, **155**, pp. 69-81, 2013.

[4] Han, D., Cau, G., McCallum, J. & Song, X., *Residence Times of Groundwater and Nitrate Transport in Coastal Aquifer Systems: Daweijia Area, Northeastern China*, Science of The Total Environment, **538**, pp. 539-554, 2015.

[5] Islami, N., *Geolectrical Resistivity and Hydrogeochemical Contrast between the Area that has been Applied with Fertilization for Long Duration and Non-Fertilization*, ITB J. Eng Sci., **42**(2), pp. 151-164, 2010.

[6] Kim, Y., Seo, Y., Kraus, D., Klatt, S., Haas, E., Tenhunen, J. & Kiese, R., *Estimation and Mitigation of N_2O Emission and Nitrate Leaching from*

Intensive Crop Cultivation in the Haean Catchment, South Korea, Science of The Total Environment, **529**, pp. 40-53, 2015.

[7] Otero, N., Torrentó, C., Soler, A., Menció, A. & Mas-Pla, J., *Monitoring Groundwater Nitrate Attenuation in a Regional System Coupling Hydrogeology with Multi-Isotopic Methods: The Case of Plana de Vic (Osona, Spain)*, Agriculture, Ecosystems & Environment, **133**(1-2), pp. 103-113, 2009.

[8] Zang, Y., Li, F., Zhang, Q., Li, J. & Liu, Q., *Tracing Nitrate Pollution Sources and Transformation in Surface- and Ground-Waters using Environmental Isotopes*, Science of The Total Environment, **490,** pp. 213-222, 2014.

[9] Al-Charideh, A. & Hasan, A., *Use of Isotopic Tracers to Characterize the Interaction of Water Components and Nitrate Contamination in the Arid Rasafeh area (Syria)*, Environ Earth Sci., **70**(1), pp. 71–82, 2013.

[10] Karan, S., Kidmose, J., Engesgaard, P., Nilsson, B., Frandsen, M., Ommen, D.O.A., Flindt, M.R., Andersen, F.Ø. & Pedersen, O., *Role of a Groundwater–Lake Interface in Controlling Seepage of Water and Nitrate*, Journal of Hydrology, **517**, pp. 791-802, 2014.

[11] Kneisel, C., Emmert, A. & Kästl, J., *Application of 3D Electrical Resistivity Imaging for Mapping Frozen Ground Conditions Exemplified by Three Case Studies*, Geomorphology, **210**, pp. 71-82, 2014.

[12] Tsokas, G.N., Tsourlos, P.I., Vargemezis, G.N. & Pazaras, N.Th., *Using Surface and Cross-Hole Resistivity Tomography in an Urban Environment: An Example of Imaging the Foundations of the Ancient Wall in Thessaloniki, North Greece*, Physics and Chemistry of the Earth, **36**(16), pp. 1310-1317, 2011.

[13] Sengul, O., *Use of Electrical Resistivity as an Indicator for Durability*, Construction and Building Materials, **73**, pp. 434-441, 2014.

[14] Chen, C-T., Chang, J-J. & Yeih, W-C., *The Effects of Specimen Parameters on the Resistivity of Concrete*, Construction and Building Materials, **71**, pp. 35-43. 2014.

[15] Sebastian, K., Maciej, M. & Piotr, T., *Determination of the Correlation between the Electrical Resistivity of Non-Cohesive Soils and the Degree of Compaction*, Journal of Applied Geophysics, **110**, pp. 43-50, 2014.

[16] Khaki, M., Yusoff, I. & Islami, N., *Groundwater Quality Assessment of a Freshwater Wetland in the Selangor (Malaysia) Using Electrical Resistivity and Chemical Analysis*, Water Science & Technology: Water Supply, **14**(2), pp. 255-264, 2014.

[17] Auken, E., Doetsch, J., Fiandaca, G., Vest Christiansen, A., Gazoty, A., Cahlil, A.G. & Jakobsen, R., *Imaging Subsurface Migration of Dissolved CO_2 in a Shallow Aquifer Using 3-D Time-Lapse Electrical Resistivity Tomography,* Journal of Applied Geophysics*,* **101**, pp. 31-41, 2014.

[18] Park, S., Yi, M-J., Kim, J-H. & Shin, S.W., *Electrical Resistivity Imaging (ERI) Monitoring for Groundwater Contamination in an Uncontrolled Landfill, South Korea*, Journal of Applied Geophysics, **135**, pp. 1-7, 2016.

[19] U.S. Environmental Protection Agency, *Nitrogen-ammonia/nitrite /nitrate, Water Quality Standards Criteria Summaries,* Washington, DC, 1980. GPO: 1980-341-082/107

[20] Noor, I.M., *Pre Feasibility Study of Potential Groundwater Development in Kelantan, Malaysia,* (Unpublished PhD Thesis), University of Birmingham, United Kingdom, 1979.

[21] Hamlin, W.K., *Earth Dynamic Systems*, Sixth Edition, Bringham Young University, Provo, Utah, 1991.

[22] Van Hoorn, J.W., *Determining Hydraulic Conductivity with the Inversed Auger Hole and Infiltrometer Methods*, Paper 1.06, pp.150-154, 1979, http://www.samsamwater.com/library/DETERMINING_HYDRAULIC_CONDUCTIVITY_WITH_THE_INVERSED_AUGER_HOLE_AND_INFILTROMETER_METHODS.pdf, accessed, 14 March 2011.

[23] Tiwari, A.K., Singh, A.K. & Mahato, M.K., *Environmental Hydro-geochemistry and Groundwater Quality*, Lambert Academic Publishing, 64 pp., 2015.

[24] Lee, M.S., Lee, K.K., Hyun, Y., Clement, T.P. & Hamilton, D., *Nitrogen Transformation and Transport Modeling in Groundwater Aquifers*, Ecol. Model, **192**(1-2), pp. 143-159, 2006.

[25] Loke, M.H., *Rapid 2-D Resistivity & IP Inversion Using the Least-squares Method,* Geotomo Software, Malaysia, 2007.

[26] Hillel, D., *Environmental Soil Physics*, San Diego, United States, Academic Press, 1998.

[27] World Health Organization (WHO), *Guideline for Drinking-water, Vol. 1, Recommendations*, Geneva, 1984.

[28] Islami, N., Taib, S., Yusoff, I. & Ghani, A.A., *Time Lapse Chemical Fertilizer Monitoring in Agriculture Sandy Soil*, International Journal of Environmental Science and Technology, **8**(4), pp. 765-780, 2011.

[29] Silva, R.G., Holub, S.M., Jorgensen, E.E. & Ashanuzzaman, A.N.M., *Indicators of Nitrate Leaching Loss Under Different Land Use of clayey and Sandy Soils in Southeastern Oklahoma*, Agriculture, Ecosyst. Environ, **109**(3-4), pp. 346-359, 2005.

[30] Hounslow, A.W., *Water Quality Data: Analysis and Interpretation*, CRC Lewis Publishers, Boca Raton, FL, United States, 1995.